Frequency Measurement in protective relays and impact by Renewable Energy Resources

Tirath Bains, Ilia Voloh, Venkatesh Chakrapani

Abstract-- **Frequency measurement algorithms implemented in the numerical relays today have largely been based on the behavior of conventional transmission system where rapid changes to frequency are not expected. The increasing penetration of renewable energy resources, especially inverter-based resources (IBRs) is resulting in lower system inertia. Though the grid codes and standards are moving in the direction of requiring IBRs to provide the 'synthetic' inertia through the means of Active Power Fast Frequency response, however, the response time and accuracy of such techniques itself depends on the speed and precision of frequency measurement algorithm within IBR controllers. In the nutshell, the faster and non-linear frequency excursions are expected and are observed in the grids with the higher penetration of IBRs. IEEE 2800 standard acknowledges frequency excursions during/after the fault in the grids dominated by IBRs and is defining frequency response requirement following the disturbances. IBRs and protective relays are expected to adhere to these requirements and ensure operation within defined margins.**

This paper identifies the challenges and discusses the improvements that can be made to the frequency measurement algorithms of the protective relays due to increasing penetration of IBRs. In this paper, firstly the frequency related challenging scenarios observed in the simulation of a power system with high integration of IBRs and real-life cases have been illustrated. Secondly, the implications of these challenges on the frequency measurement algorithm and consequently, the impact on the protection and control actions of frequency protection is also discussed. Thirdly, the prospective changes to the frequency measurement algorithm have been identified based on the presented detailed mathematical analysis. We then introduce the enhancements to the legacy frequency measurement algorithm. A thorough evaluation of the improved frequency measurement algorithm is performed, using both real field cases and simulated signals with real controller.

I. Introduction

Frequency is generally understood as number of repetitions of an event over a specific time period. In power systems, frequency is the number of cycles per second (Hz) completed by the voltage or current signals. In conventional power systems the power source was almost invariably a synchronous generator. Therefore, the frequency of voltage and current waveforms was dictated by the rotating speed of the synchronous generator i.e.,

$$f_e = f_m * \frac{P}{2} \quad (1)$$

where f_e represent electrical frequency of power system (voltage/current signal frequency); f_m represents mechanical frequency of the synchronous generator rotor; P is the number of poles of the synchronous generator.

Since, the frequency of the voltage and current waveforms is closely related to the rotational speed of the generator, the frequency measured from voltage/current signals provides us with very critical information the state of balance between power generation and consumption. The decrease in frequency from its nominal value or Under-frequency (UF) condition indicates that the synchronous generator is slowing down, indicating that the power consumption is higher than the power generation. The system operator can therefore take the corrective action of increasing the power generation or shedding the load. The increase in frequency or Over-frequency (OF) condition implies that synchronous generator is speeding up indicating higher power generation than the consumption, and the operator could curtail the generation as corrective action. The Rate of Change of Frequency (RoCoF) as the name suggests measures the rate at which frequency is changing with respect to the time. RoCoF indicates the pace of the imbalance that is occuring between power generation and consumption. Higher the value of RoCoF, the faster is the pace with which the balance between generation and consumption is deteriorating. If the RoCoF is negative the operator can shed the load or increase the generation, and if the RoCoF is positive then operator can curtail the generation. The overexcitation protection (V/Hz) for generators and transformers is another application where accurate information is required.

Apart from the frequency relaying, accurate estimation of frequency is very important for accurate phasor estimation. An error in frequency estimation induces an error in the phasor estimation, which results in deterioration of the phasor-based protection and control functions.

From the above discussion, it becomes clear that frequency of the system provides very critical information about the system health. Since, the voltage and current frequencies are closely related to the frequency of the synchronous generators, the voltage and current signals have been widely used to measure the system frequency.

In the recent years the contribution from renewable energy resources, including inverter-based resources (IBRs) have significantly increased. The IBRs produce sinusoidal voltage and currents by using the power electronics interface. The response of an IBR to any disturbance depends upon the control design of the power electronics interface, which could be different based on the manufacturer, type of IBR (wind, solar, battery energy etc). It is in contrast to the standard design of the synchronous generator of the conventional system.

This paper investigates the effect of high-level penetration of IBRs on the frequency response of the power system and the

frequency measurement of the protective relays. Firstly, the types of signals used for frequency estimation and the most commonly used frequency estimation algorithms are presented in Section II. In Section III, the various issues that arise during frequency estimation in IBR dominated grid are presented using the PSCAD simulation. PSCAD simulation uses the models of the real controllers employed in the field for various types of IBRs. The conclusions of the paper are presented in Section IV.

II. Frequency Estimation Algorithms: An overview

A. Commonly used signals to estimate frequency

The frequency can be estimated from any of the followings power system signals:

- single-phase voltage
- Clarke's-transform of three-phase voltage
- auxiliary voltage
- single-phase current
- Clarke's-transform of three-phase current
- neutral current

Generally, voltage signal is used for frequency estimation as it is a stationary signal at steady state, i.e., amplitude and frequency remain constant during normal operations, and is less affected by transient and harmonics during the system disturbances. The Clarke's transform of three-phase voltage has additional benefit that it provides a robust signal during single or double phase contingencies like faults, open pole, VT fuse failure. On the other hand, the magnitude of the current changes frequently and usually has higher harmonic content. However, there remain cases where only current waveforms might be available for frequency measurement, such as line differential and bus differential relays. Therefore, in this paper the frequency is estimated using both voltages and currents.

B. Commonly used algorithms to estimate frequency

1) Zero Crossing

The frequency of a periodic signal can be estimated by measuring the time period between zero-crossings. Zero-crossing can be identified by the change of the sign of a sample as compared to the previous sample (positive to negative or negative to positive). The actual point of zero-crossing can be obtained by linear interpolation as shown in Figure 1.

The frequency can be estimated from the zero-crossing timestamps as follow:

$$f_{est} = \frac{1}{T_3 - T_1} = \frac{0.5}{T_2 - T_1} \qquad (2)$$

Where T1 and T3 are the zero-crossing timestamps when signal transitions from negative to positive and are mutually one cycle apart. T2 is the zero-crossing time stamp when signal transition from positive to negative. T2 is separated by half-cycle from T1 and T3. As seen from eq (2), the frequency can be estimated once a cycle if timestamp T1 and T3 are used or twice a cycle if timestamps T1 and T2 or T2 and T3 are used. It is obvious that accuracy of the localization of a zero-crossing could be affected by the presence of the harmonics, noise, transients or other distortions. Therefore, a low pass filter can be applied to reduce the effects of harmonics and noise. The step changes in the phase of a voltage/current waveform can lead to few erroneous/unrealistic frequency readings, therefore, to further improve the accuracy of zero-crossing based methods, the post-filtering might be applied.

Zero-crossing method can provide frequency measurement only after half or a full cycle delay. Various techniques can be found in literature such as [1], [2] which aim to enhance the dynamic behavior of Zero-crossing method. Nevertheless, Zero-crossing method remains the most widely used algorithm owing to its simplicity.

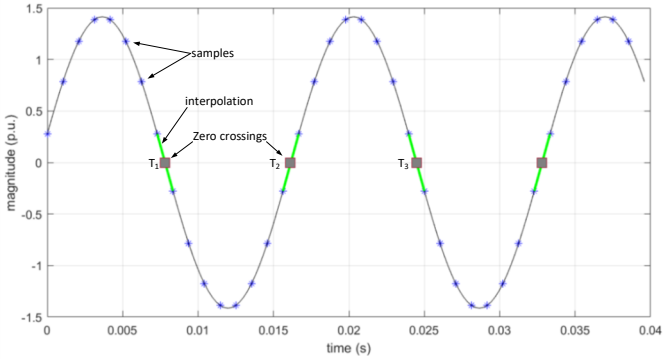

Figure 1: Detecting Zero-crossing based on linear interpolation.

2) Discrete Fourier Transform (DFT) based method

DFT is commonly used for calculating voltage and current phasors. For a discrete signal *v(k)* if a fundamental frequency cycle contains exactly N samples, then the phasor of fundamental frequency is obtained by the following expression:

$$\overline{V}(k) = \frac{2}{N}\sum_{n=0}^{N-1} v(k+n-N+1)\, e^{-\frac{j2\pi n}{N}} \qquad (3)$$

$\overline{V}(k)$ is a phasor quantity with magnitude equal to the peak value of the signal and its phasor angle (φ) rotating with respect to time (t) as per: $\varphi = 2\pi f t + \varphi_o$, where f represents the fundamental frequency, φ_o represents the initial phase angle at t=0.

As an example, consider, a 60Hz signal shown in Figure 2(a). It can be seen that the phasor angle $\varphi(t)$ as calculated by the DFT of the sine wave is varying linearly with respect to time (see Figure 2(b)). The fundamental frequency of the signal thus can be obtained by taking derivative of $\varphi(t)$:

$$f_{est} = \frac{1}{2\pi}\frac{d\varphi}{dt} \quad (4)$$

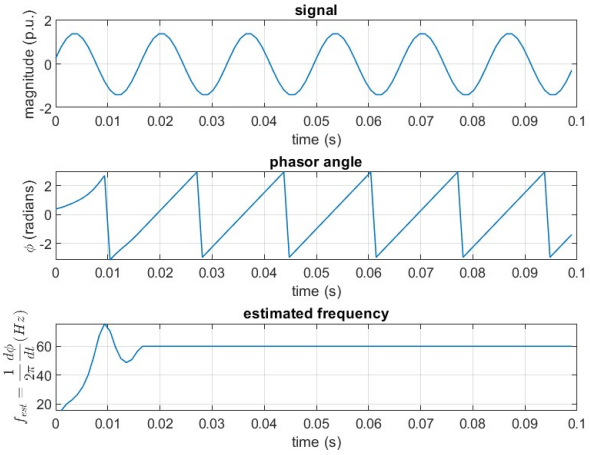

Figure 2: Frequency as derivative of the phasor angle yielded by DFT

The equation (4) only holds true if the one cycle of fundamental frequency contains exactly N samples per cycle. The off-nominal frequencies will not contain exactly N samples per cycles and thereby resulting in errors in phasor estimation (magnitude as well as phasor angle) which in-turn affects the accuracy of the frequency estimation.

To eliminate this error various approaches have been proposed, the main of which are:

- Adaptive sampling rate: the sampling rate is updated according to the estimated frequency, so that the number of samples per cycle of the signal frequency remain constant. Carefully designed feedback is required to achieve higher accuracy with acceptable latency.
- Adaptive DFT window length: the sampling rate remains fixed but the number of samples per cycle of the signal frequency are changed. Feedback loop is required to update the DFT window length based upon the measured frequency. Still, it is not guaranteed that updated DFT window length will contain exactly one cycle of the signal frequency.
- Resampling: the received samples are resampled so that one cycle of signal frequency contains exactly the fixed number of samples. This approach is similar to adaptive sampling rate, but with key difference being that resampling is done at software level while in adaptive sampling rate the sampling rate is changed at the hardware level. Feedback loop will be required to resample the received samples as per the estimated frequency.
- Analytical compensation of error: With fixed sampling rate and fixed DFT window length, this approach aims to find the error that would be incurred in the calculated phasor when the signal frequency deviates from the nominal frequency and then compensate it. The frequency is then calculated from the corrected phasor.

In this paper analytical approach presented in [3] has been used.

3) Signal demodulation

It is known fact that when two sinusoidal signals are multiplied, the result can be represented as the summation of two sinusoids with frequency of one sinusoid being the summation of the frequencies of the original signals, while the frequency of the other sinusoid will be the difference of the frequencies of the original signals. Mathematically, it can be represented as follows:

$$A\cos(2\pi f_0 t + \varphi_o).\cos(2\pi f_1 t) = \frac{A}{2}[\cos(2\pi(f_0 - f_1)t + \varphi_o) + \cos(2\pi(f_0 + f_1)t) + \varphi_o] \quad (5)$$

In signal demodulation method (SDM), the measured signal (v_i) is multiplied by the nominal frequency as shown in Figure 3. It results in the signal (v_m) which has a low frequency and near double frequency as per eq (5). Then the high/double frequency component is removed using low-pass filter with residue containing the signal (v_o) whose phase angle is rotating with a frequency which is equal to the difference between nominal frequency and actual frequency. The actual frequency is estimated based on the rotating speed of the signal v_o. In this paper SDM is modelled using the approach given in [4].

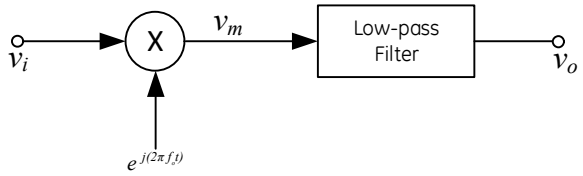

Figure 3: Schematic diagram showing the working principle of SDM method.

As an example, consider measuring a 55Hz signal using SDM. Figure 4(a) shows a 55Hz signal used to estimate the frequency. Figure 4(b) shows the real and imaginary part of the modulated signal. Figure 4(c) shows the real and imaginary part of the low-pass filtered signal. Note the near double frequency and low frequency (5Hz) components in the modulated signal but only low frequency component in the filtered signal. The Figure 4(d) shows the estimated frequency using SDM.

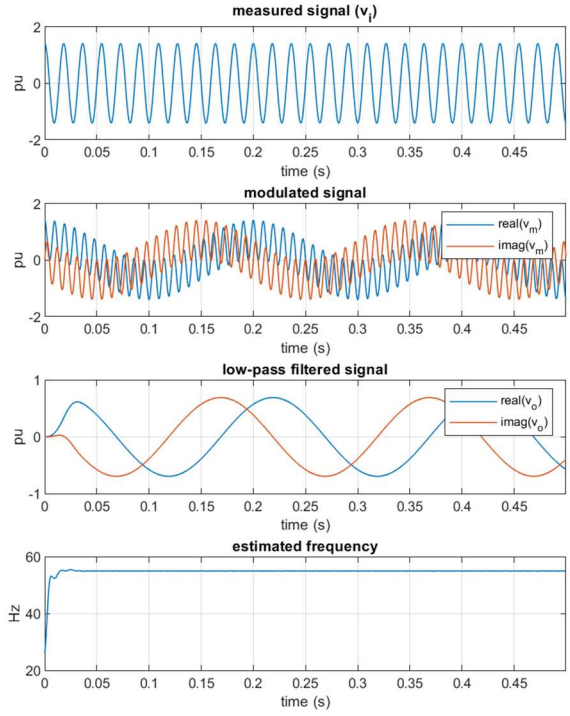

Figure 4: Example of SDM method of frequency estimation (a) 55Hz waveform, (b) modulated signal with a near-double frequency and low-frequency, (c) low pass filtered signal containing only low frequency, (d) estimated frequency

III. IBRs AND FREQUENCY MEASUREMENT ISSUES

The synchronous generators have been in-service in the power systems for several decades and their design has remained consistent across the globe. Therefore, the response of synchronous generator and consequent effect on system frequency due to a fault or other disturbances is well understood. Additionally, the synchronous generators have massive rotating inertia associated with them and the turbine and excitation control systems are relatively slow, which lets the system ride through disturbances with very limited frequency excursions.

Now on the other hand, IBRs are connected to the grid through a power electronics interface. The control design for power electronics interface varies from vendor to vendor and from the type of the IBR (wind: Type3 or Type4, solar). For example, the stator winding of the Type3 wind turbine is coupled directly to the power system while rotor is connected through power electronics interface. On the other hand, in Type4 wind turbines the rotor and stator windings are connected through power electronic interface. Similarly, solar is connected to power system through power electronics interface. Moreover, IBRs do not have rotating inertia associated with them and the control systems for power electronics devices are fast acting, which can produce faster frequency changes as compared to synchronous generator dominated systems. Thus, it is expected that the effect of IBRs on frequency due to system disturbances/faults will vary on case-by-case basis, depending upon the type of IBR control used, and possibly due to IBR manufacturer. This fact highlights the need for standards to regulate the frequency response of an IBR following a disturbance in the system. Moreover, the standards are not explicitly clear on the frequency measurement algorithms, such as type of algorithm, length of measurement window, latency, pre-filtering and post-filtering etc.

To study the impact of IBRs on the frequency estimation, a 230kV system shown in Figure 5 was simulated in PSCAD. The PSCAD simulation utilizes the model of real commercially available controllers employed in the field for different types of IBRs which are: 1-Type-3 wind turbine generator (WTG); 2-Battery energy storage system; 3-Type-4 off-shore WTG.

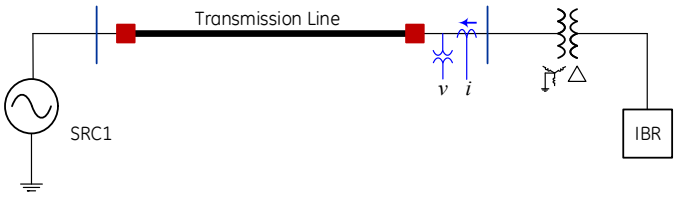

Figure 5: Schematic of the system modeled in PSCAD.

The transmission line is rated at 230kV and is modelled using frequency dependent model with total length of 50 km. The positive and zero-sequence impedances of the transmission line are *(0.0347+0.4234j) Ω/km* and *(0.3+1.1426j) Ω/km*. The transmission line is not ideally transposed. The source is modelled using a voltage source with internal impedance. The internal impedance of the source is changed to obtain different levels of Source impedance ratios (SIR) of 0.5, 1, 5. Usage of the different SIRs on LHS side provides the different penetration level of IBRs in the system. The current and voltage waveforms analyzed in this paper are recorded at the IBR side of the transmission line.

A. Pre-filter of the signals

In conventional systems, the voltages are largely sinusoidal with very limited amount of harmonics or other higher frequencies. Even during a fault or any disturbance the voltages remain largely sinusoidal. However, IBR dominated systems require relatively larger harmonic filters, otherwise the voltages are likely to have higher content of harmonics.

Figure 6 shows the voltage waveforms recorded from a system with conventional source under steady state, and the estimated frequency by zero crossing (ZC) and DFT methods without applying any filtering of the voltages. The signal demodulation (SDM) method is not shown because filtering is inherently applied in SDM. It can be observed that the estimated frequency by ZC and DFT methods is accurate and with virtual no excursions. The voltage waveforms are remarkably clean.

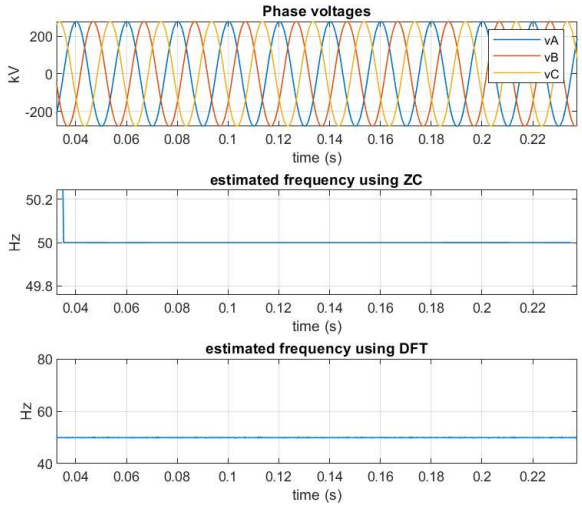

Figure 6: Estimated frequency by ZC and DFT methods (without filtering) in a conventional system.

Figure 7 shows the phase voltages recorded from a system dominated by IBRs under steady state, and the estimated frequency using ZC and DFT methods without applying any filtering on the voltage waveforms. It can be observed that frequency estimated by ZC and DFT methods shows oscillatory behavior especially the DFT. The reason for relatively fast and larger oscillations specifically in DFT method is that DFT method is susceptible to harmonics and noise in the signal [5]. The oscillatory behavior of estimated frequencies is due to the presence of high frequency components presents in the voltage waveforms, which can be observed on careful observation of the waveforms shown in Figure 7. Note that the system is under steady state operation.

Figure 8 shows the estimated frequency for the voltage waveforms from IBR dominated system with the application of a low band pass filter. The oscillatory behavior of estimated behavior has been significantly using a low band pass filter.

It can thus be concluded that that applying low pass or low pass band filtering is strongly recommended for estimating frequency in IBR-dominated systems. The low band pass filtering is applied for ZC and DFT methods in all the cases presented in this paper, hereafter.

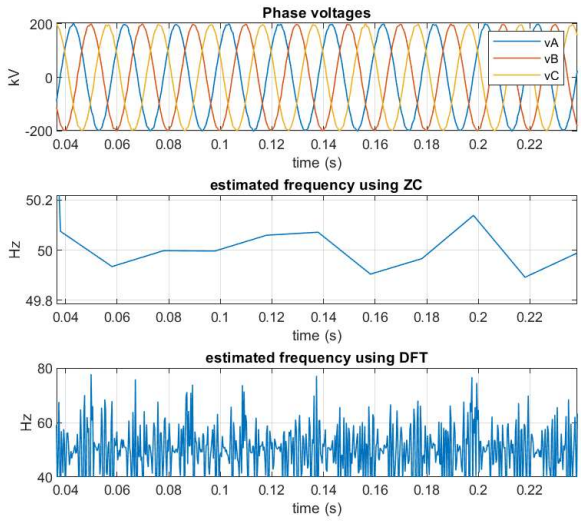

Figure 7: Estimated frequency by ZC and DFT methods (without filtering) in an IBR-dominated system.

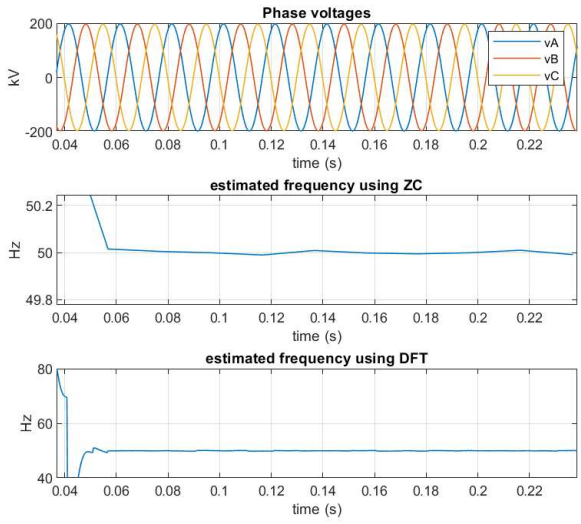

Figure 8: Estimated frequency by ZC and DFT methods (with low bandpass filtering) in an IBR-dominated system.

B. Type of frequency measurement algorithm

Figure 9 shows the recorded voltage and current waveforms for a solid phase-A to ground fault at the remote terminal of the transmission line as seen from IBR terminal, and the estimated frequencies from voltage and current using 3 different algorithms. The type of IBR is WTG Type-3.

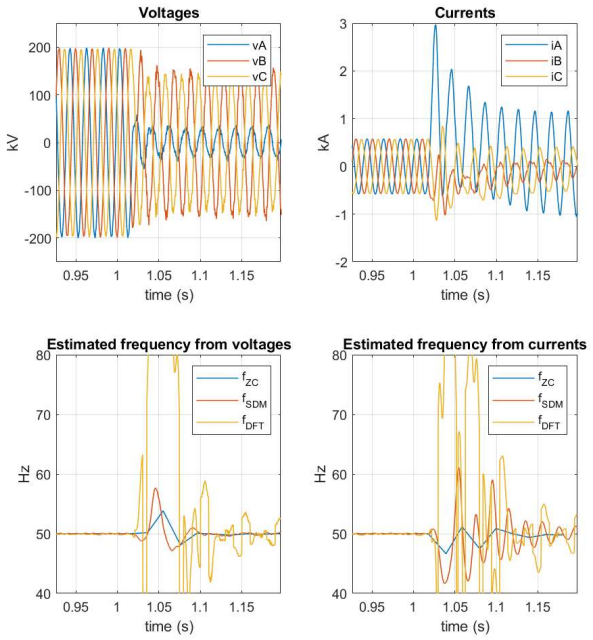

Figure 9: Voltage and current waveforms for a solid phase-A to ground fault and estimated frequency from voltages and currents.

It can be observed that the frequency estimated by DFT method (represented by f_{DFT}) shows relatively very large frequency excursions as compared to the ZC and SDM methods (represented by f_{ZC} and f_{SDM}, respectively). This is due to the fact that DFT method is a 'short window' method which aims to estimate the frequency component from the 3 consecutive phasor measurements, assuming that there is only frequency component in the signal. It makes DFT method to be very responsive to the instantaneous value of frequency but at the same time very sensitive to transients, harmonics, and noise in the signal. It is possible to adapt DFT algorithm to multiple frequencies in the system, however, the equations become cumbersome and relatively high computational power would be required to solve the equations numerically. It should be noted that a low pass filter is applied to the raw signal to filter out higher frequencies before applying to the DFT method.

The ZC and SDM methods are essentially 'long-window' methods because: ZC makes frequency reading only when zero-crossing is detected, irrespective of the instantaneous values of frequency during the whole cycle, while SDM removes the higher frequency during the low-pass filtering of the modulated signal. Therefore, ZC and SDM methods produce relatively small frequency excursions.

However, these frequency excursions in ZC and SDM are relatively large as compared to the ones seen in conventional system. Therefore, the post filtering employed in frequency estimation algorithms to verify the sanity of the frequency measurement might require relaxation or it needs to be made adaptive.

It brings forward an important question for the frequency response of IBRs to a disturbance or a fault. How the frequency should be interpreted by the IBR manufacturers, when there are multiple ways to estimate a frequency with each method providing different results.

C. System strength and frequency estimation

The Figure 10 shows the recorded voltage and current waveforms for a phase-A to phase-C fault at the remote end of the transmission line as seen from the IBR side. The type of IBR is type-3 WTG, and the SIR of the source on LHS is 1.

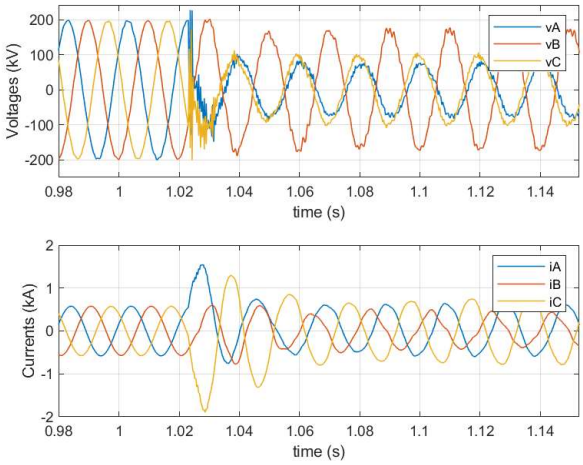

Figure 10: Voltage and current waveforms for an AC fault in a system with SIR=1 coupled to a Type-3 WTG.

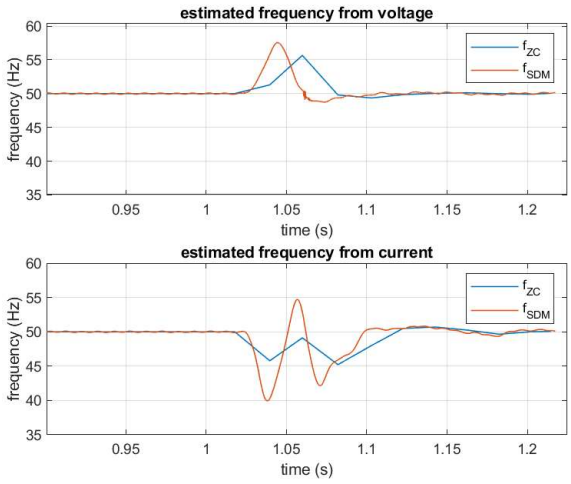

Figure 11: Estimated frequency from voltages and currents for an AC fault in a system with the SIR of the source on LHS=1, coupled to a Type-3 WTG.

It can be seen from Figure 10 that following the fault a considerable amount of high frequency transients is present in voltage waveforms. It is therefore imperative for the zero-crossing based frequency estimation to employ low-pass or a band-pass filter to filter out high frequency transients. On the other hand, the behavior of the current is markedly non-linear for approximately two cycles following the fault especially the time period between 1.04s to 1.06s. Since frequency measurement algorithms estimate frequency based on rate of change of the phase of the waveform, this non-linearity is expected to produce frequency excursions well-outside the expected range.

Figure 11 shows the estimated frequency from voltage and

current waveforms for the above case using ZC and SDM methods. It can be seen that frequency measured from the voltage changes abruptly due to the step change in the phase of the voltage due to the fault, and then it settles close to the nominal value within 2 cycles. The frequency estimated from the current waveform shows relatively larger and longer frequency excursions.

To understand the effect of increasing IBR penetration on frequency estimation the same fault scenario as previous case (same fault type, location, point on wave and resistance) except that the SIR of the source on LHS is increased to 5, i.e., IBR is coupled to weaker system in this case. Figure 12 shows voltage and current waveforms for this case. It can be observed that high frequency component in the voltage waveforms has become significantly larger as compared to the previous case. The non-linearity in the current waveforms for couple of cycles after fault has become more pronounced.

Figure 13 shows the estimated frequency from voltage and current waveforms for this case which shows that the frequency excursions are larger and last relatively longer as compared to the previous case. However, the frequency estimated using voltages is relatively less affected as compared to the frequency estimated using currents. This observation highlights the fact that the voltage at IBR terminals is predominantly governed by the grid while the current injected by IBR depends upon the control design and operating mode. Therefore, voltage waveforms are a better choice for frequency estimation in grids dominated by IBRs.

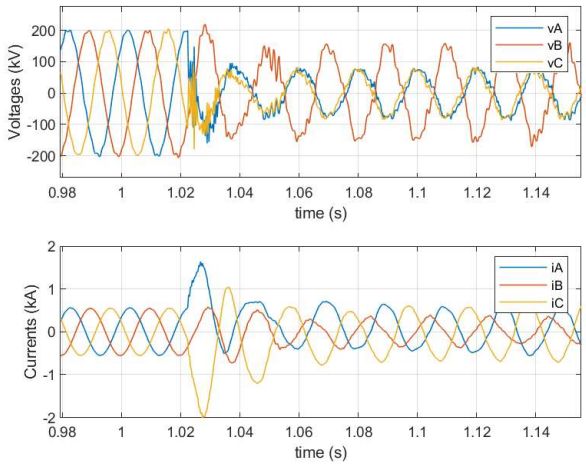

Figure 12: Voltage and current waveforms for an AC fault in a system with SIR of the source on LHS=5 coupled to a Type-3 WTG.

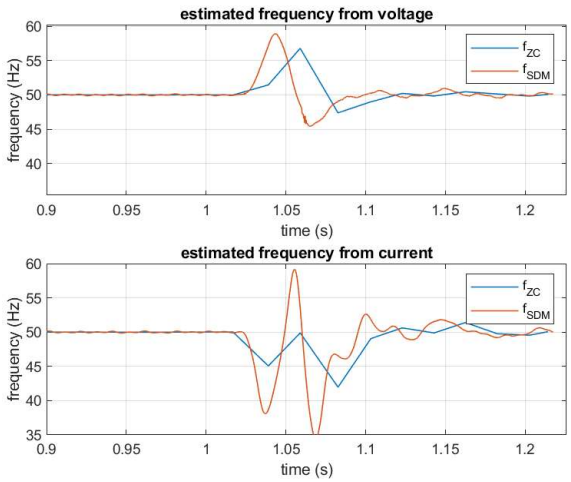

Figure 13: Estimated frequency from voltages and currents for an AC fault in a system with SIR=5 coupled to a Type-3 WTG.

It is worth noting that the grid in the simulation is represented by a sinusoidal voltage source which has 'infinite' rotating inertia and can maintain voltage frequency at nominal value. However, in case of a real system with high level of IBR penetration, the grid might not be able to maintain voltage frequency close to its nominal value due to its limited rotational inertia.

D. IBR type and current frequency estimation

As previously noted, the voltage frequency is largely dictated by the grid, however, the current frequency will depend upon the control design and operating mode. Therefore, voltage becomes the primary choice for estimating grid frequency. However, current frequency becomes crucial when voltages are not available for frequency estimation such as in line and bus differential relays.

Figure 14 shows the recorded current waveforms for a same fault scenario with different type of IBRs in the system. The fault case under consideration close-in forward phase-A to phase-B solid fault with type of IBR being used: (a) WTG Type-3, (b) WTG Type-4 (Offshore), (c) BESS Type-4. The outline, the amount of high frequency components, the non-linearity of current waveforms is different in each case, especially immediately after the fault inception. Figure 15 shows the frequency measured from the currents in each case using ZC and SDM methods. A wide divergence in the frequency measurements immediately after the fault inception can be observed in each case. However, after about 100ms after the fault inception the frequency measurements start converging on the final 'steady-state' measurements. This is inline with the observation made in [6], that after the disturbance detection and control system transient period is over, the IBR behavior reaches 'steady-state' fault behavior.

Thus, when frequency is estimated from currents, using the delayed frequency measurements would be more accurate for frequency relaying instead of the frequency measurements immediately following the fault.

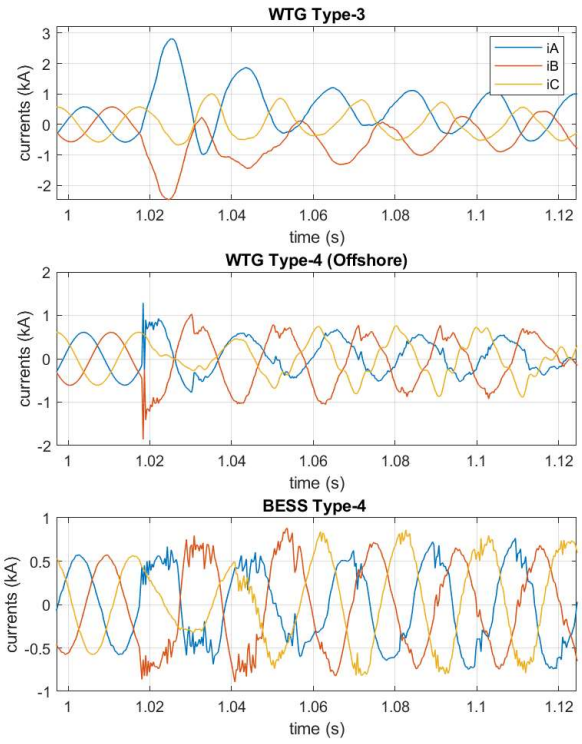

Figure 14: The recorded phase current waveforms for a solid phase A to phase-C, close-in forward fault at the IBR terminal of the transmission line for different types of IBRs.

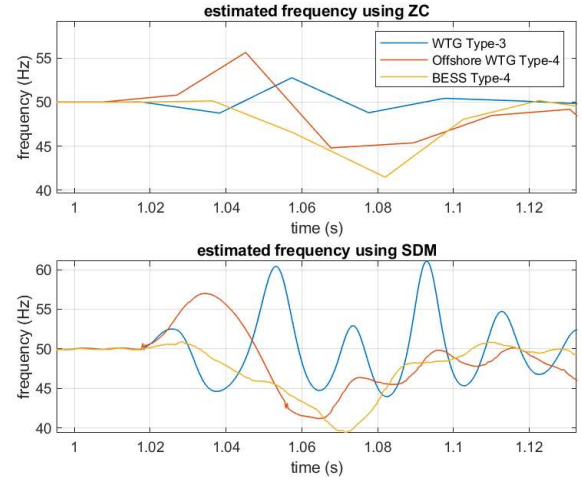

Figure 15: The estimated frequency following a solid phase A to phase-C, close-in forward fault at the IBR terminal of the transmission line for different types of IBRs.

E. Real field case

Figure 16 shows the current and voltage waveforms from real field case of a 3-phase fault from a grid dominated by IBRs. By observing the voltage waveform, we can clearly identify four different operating behavior of the system:

1. Pre-fault
2. A 3-phase fault which is cleared about 120ms later
3. A period of duration of approximately 150ms with relatively higher frequency than the nominal frequency and considerable non-linear behavior.
4. 'Ramping-down' of the voltage magnitude with a stable frequency.

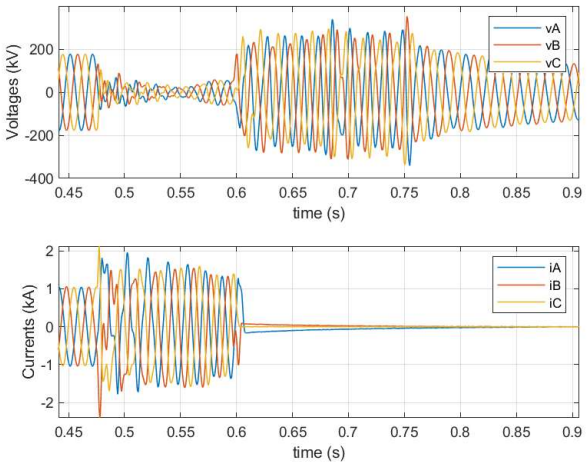

Figure 16: Voltage and current waveforms for from real field case of a 3-phase fault in grid dominated by IBRs.

Figure 17 shows the frequency measured from voltage and currents for this case. It can be seen from Figure 17 that the voltage and current frequencies rise rapidly following the inception of the fault. When the fault gets cleared the current becomes zero and as a result current frequency becomes zero.

On the other hand, the voltage frequency drops momentarily to about 55Hz and then rises to about 70Hz within next 50-100ms. Thereafter, the voltage frequency briefly 'levels-off' at about 65Hz for approximately 50ms which is then followed by quick ramping down to its final value of approximately 45Hz.

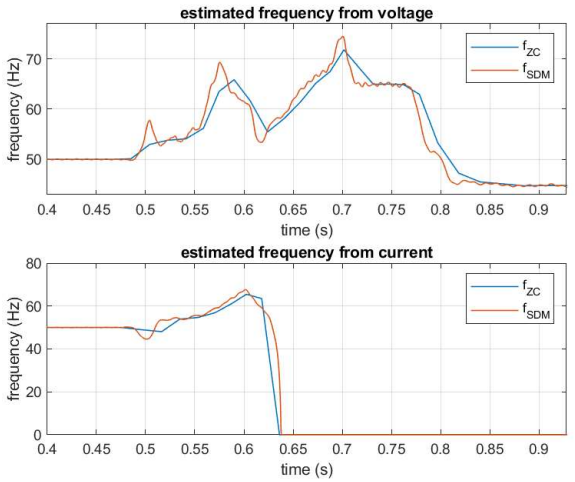

Figure 17: Estimated frequency from voltages and currents for a 3-phase fault in grid dominated by IBRs.

From Figure 17, it can be seen that system frequency changed from its nominal value of 50Hz to about 70Hz and then finally settling at 45Hz, all with-in a span of 300ms. It shows that very fast and wide frequency excursions occur in the system dominated by IBRs. This brings forth the effect of such fast excursions on the Rate of Change of Frequency (RoCoF) element.

RoCoF element is very sensitive to the change in estimated

frequency. The change could be the real organic change or an error in the frequency measurement. Figure 18 shows the calculated value of RoCoF for the real case shown in Figure 16. RoCoF is calculated by averaging the frequency over a 4-cycle window as well as with-out averaging. It can be seen that when frequency is not averaged, the RoCoF values in the range of 400-500Hz/s are observed. When the RoCoF is measured from averaged frequency over 4-cycle the RoCoF values still remain in the range of 100-300Hz/s. The question arises what is the significance of such large RoCof values? Is it an actionable input or is it a mere transient behavior and that RoCoF based decision should be delayed letting RoCoF values settle?

It highlights the 'double-duty' that is required of the frequency measurement algorithms with regards to the sanity check. Firstly, the sanity-check has to be ascertained that whether the frequency measurement is credible or not. Secondly, its has to be ensured that the any valid frequency is not rejected by sanity-check, given the wide frequency excursions observed in IBR-dominated systems.

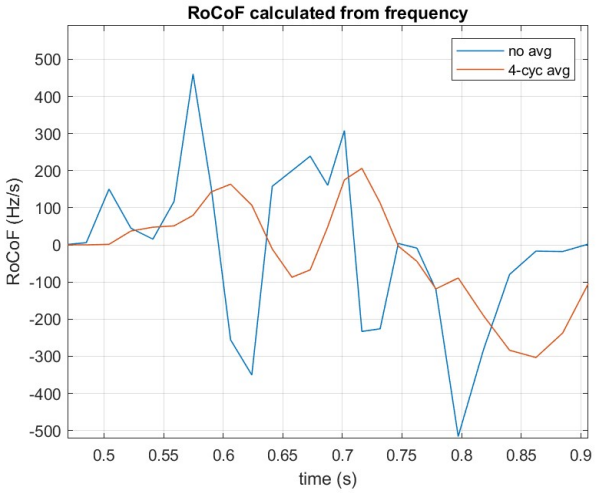

Figure 18: Rate of Change of Frequency (RoCoF) calculated using frequency estimated from voltages using ZC method.

F. Findings and Recommendations

Following are the findings and the recommendations for estimating the frequency in the system dominated by IBRs based on this paper:

1. Low pass or low band pass filtering is strongly recommended/critical for frequency measurements due to high frequency components in the voltage and currents signals near IBRs.
2. The frequency estimation techniques that are aimed at providing instantaneous value of the frequency are likely to produce larger frequency excursions as compared to the techniques which provide frequency measurement over a window of time. A careful examination and selection of the frequency estimation technique must be made.
3. Larger frequency excursions during disturbances are expected in a weaker system as compared to the stronger system. Voltages are relatively less affected than current.
4. The type of the IBR type and control mode used could affect the accuracy of the frequency measurement from the current waveforms immediately following the inception of a fault. This is due to the different transient behavior of the control system. The control system reaches 'steady-state' normally in 5-6 cycles.
5. Standard acknowledges that IBR frequency response may not be accurate especially at the beginning of the disturbance.
6. ROCOF estimation depends crucially upon the post-filtering of the frequency measurements. Sanity check of frequency measurements has 'double duty' in IBR-dominated systems, i.e., to discard erroneous frequency measurements while accommodating larger possible frequency excursions in IBR-dominated systems.

IV. Conclusion

This paper presented the basics of frequency estimation, the commonly used methods, and signals for the frequency estimation. The various challenges that will be encountered while estimating frequency in the IBR-dominated systems have been presented in this paper through PSCAD simulation. The model of real commercially available controllers employed in the field have been used in PSCAD simulation, providing the results which would emulate real cases in the field. Based on the observations from the simulation, the recommendations regarding the pre-filtering, post-filtering, type of frequency estimation method, advantages, limitations of using voltage vs. currents waveforms for estimating frequency have been discussed.

IEEE 2800 standard does not require frequency or change of frequency protection for the IBR plant itself, but frequency protection still can be used for the system protection and can be deployed in the vicinity of the IBR plant.

However, protective relays performance deployed in the vicinity of the IBR plant can be affected by the erroneous frequency measurements, particularly it can affect tracking frequency and protection elements using voltage and currents which can be at different frequency during faults.

V. Acknowledgment

Authors would like to acknowledge invaluable support and hard work of GE Global Research Center.

VI. References

[1] C. T. Nguyen and K. Srinivasan. A new technique for rapid tracking of frequency deviation based on level crossing. *IEEE Trans. Power Apparatus and Systems*, 103(8):2230–2236, Aug. 1984.

[2] R. Aghazadeh, H. Lesani, M. Sanaye-Pasand, and B. Ganji. New technique for frequency and amplitude estimation of power system signals. *IEE Proc. Generation, Transmission and Distribution*, 152(3):435–440, May 2005.

[3] J. Z. Yang and C. W. Liu. A precise calculation of power system frequency and phasor. *IEEE Trans. Power Delivery*, 15(2):494–499, April 2000.

[4] P. Denys, C. Counan, L. Hossenlopp, and C. Holweck. Measurement of voltage phase for the french future defence plan against losses of synchronism. *IEEE Trans. Power Delivery*, 7(1):62–69, Jan. 1992.
[5] Spark Xue, Bogdan Kasztenny, Ilia Voloh and Dapo Oyenuga. Power System Frequency Measurement for Frequency Relaying. *Western Protective Relay Conference*, 2007.
[6] Venkatesh C, Ilia Voloh. Impact of Renewable Generation Resources on the Distance Protection and Solutions. *Western Protective Relay Conference*, 2021.

VII. BIOGRAPHIES

Tirath Bains received The B.E. degree in Electrical Engineering from Punjab Engineering College, Chandigarh, India in 2008. He completed his Master of Engineering Science and PhD degrees from The University of Western Ontario in 2014, and 2018, respectively. Since 2019 has been with GE as Lead Design Specialist in Research and Development at GE Grid Solutions, Markham, ON, Canada. His main research interest includes frequency-based and time-based protection and fault location algorithms, and high impedance fault detection algorithms.

Ilia Voloh received the Electrical Engineering degree from Ivanovo State Power University, Ivanovo, Russia. He is currently an Applications Engineering Manager with GE Grid Solutions, Markham, ON, Canada. He has authored and coauthored more than 60 papers presented at major North America Protective Relaying conferences. His areas of interest are advanced power system protection algorithms and advanced communications for protective relaying. He is a member of IEC TC95 committee and an active member of the main IEEE PSRC committee.

Venkatesh C received the B.E. degree in Electrical and Electronics Engineering from the Madras University, India, in 2004, Post Graduation in thermal power plant engineering from National Power Training Institute, Neyveli, Ministry of Power, India, in 2005 and the M.Tech. degree from the Indian Institute of Technology Delhi, New Delhi, India in 2010 and holds PhD degree from Indian Institute of Technology Madras. He worked in Delhi Discom for five years where he handled protection, SCADA, commissioning. He holds a trade secret for his invention and authored several technical papers in the area or line protection and he is a senior member of IEEE. Since 2015, he has been with General Electric, and currently holds the position of Lead Design Engineer in Research and Development at GE Grid Solutions, Stafford, United Kingdom.